Journal of Radiotherapy in Practice

Journal of Radiotherapy in Practice (2015)
14, 410–417 © Cambridge University Press 2015
doi:10.1017/S1460396915000321

Original Article

Long-term stability of the Hounsfield unit to electron density calibration curve in cone-beam computed tomography images for adaptive radiotherapy treatment planning

Akihiro Takemura[1], Shogo Tanabe[2], Mei Tokai[3], Shinichi Ueda[4], Kimiya Noto[4], Naoki Isomura[4], Hironori Kojima[4]

[1]*Institution of Medical, Pharmaceutical and Health Sciences, Faculty of Health Sciences, Kanazawa University, Kanazawa, Japan,* [2]*Department of Radiodiagnosis, Osaka Medical Center for Cancer and Cardiovascular Diseases, Higashinari, Osaka, Japan,* [3]*Division of Health Sciences, Graduate School of Medical Science, Kanazawa University, Kanazawa, Japan,* [4]*Department of Radiological Technology, Kanazawa University Hospital, Kanazawa, Japan*

(Received 14 April 2015; revised 17 June 2015; accepted 21 June 2015; first published online 15 July 2015)

Abstract

Aim: To use cone-beam computed tomography (CBCT) images for treatment planning, the Hounsfield unit (HU)-electron density (ED) calibration table for CBCT should be stable. The purpose of this study was to verify the stability of the HU values for the CBCT system over 1 year and to evaluate the effects of variation in HU-ED calibration curves on dose calculation.

Materials and Methods: A tissue characterisation phantom was scanned with the field of view (FOV) of size S (FOV-S) and FOV of size M (FOV-M) using the CBCT system once a month for 1 year. A single field treatment plan was constructed on digital phantom images to validate the dose distribution using mean HU-ED calibration curves and possible variations.

Results: HU values for each material rod over the observation period varied with trend. The HU value of the cortical bone rod decreased by about 100 HU for the FOV-S and by about 300 HU for the FOV-M. Possible variation in the HU-ED calibration curves produced a $\leq$17·9% dose difference in the dose maximum in the treatment plan.

Conclusions: The CBCT system should be calibrated periodically for consistent dose calculation.

Keywords: adaptive radiotherapy; CBCT; dose calculation; HU-ED calibration table; long-term stability

INTRODUCTION

Cone-beam computed tomography (CBCT) images are typically used for the correction of patient setup error in precision radiation therapy. Treatment planning using CBCT images for adaptive radiotherapy has been investigated by several studies.[1–5] Guan et al.[6] found that dose

Correspondence to: Akihiro Takemura, Institution of Medical, Pharmaceutical and Health Sciences, Faculty of Health Sciences, Kanazawa University, 5-11-80 Kodatsuno, Kanazawa 902-0942, Japan. Tel: +8 176 265 2538. Fax: +8 176 234 4366. E-mail: at@mhs.mp.kanazawa-u.ac.jp

calculation based on CBCT images acquired using an On-Board Imager (OBI) system (Varian Medical Systems, Palo Alto, CA, USA) had a maximum dose difference of 7% relative to the dose calculated on the planning computed tomography (CT) images. The authors of that study did not recommend the use of Catphan® phantoms (The Phantom Laboratory, Salem, NY, USA) for acquiring a Hounsfield unit (HU) to relative electron density (HU-ED) calibration curves for CBCT scanners and instead suggested the use of a dedicated phantom. They also emphasised the importance of an appropriate HU-ED calibration curve for dose calculation using CBCT images.[6]

HU values in CBCT images are affected by object size and CBCT scan conditions. Hatton et al.[7] evaluated the effects of phantom diameter and length on a HU-ED calibration curve and subsequent dose calculation. They found that differences in the phantom length resulted in a maximum difference of 260 HU, and differences in the phantom diameter resulted in a maximum difference of 1,200 HU. In addition, the calculated dose from 6 and 18 MV photon beams varied by $\leq$20% at points near bony structures. Rong et al.[8] evaluated the effects of the CBCT conditions (mAs, source-to-isocenter distance, cone angle) and phantom size (diameter and length) on dose calculation and proposed a site-specific calibration curve.

To accomplish accurate dose calculation based on CBCT images with a HU-ED calibration curve dependent on the scanning conditions and object size, the HU values based on CBCT images were transferred to appropriate HU values for dose calculations for adaptive radiotherapy in a number of studies.[2,4,5,9] However, this technique is not widely available in clinical practice, and variations in the HU value and HU-ED calibration curve may affect the accuracy of dose calculation. Further, as CBCT systems age, changes in the HU-ED calibration curve may appear.

Yadav et al.[10] investigated the stability of the HU-ED calibration curve for the Varian OBI system over the course of 6 months and found the CBCT system to be fairly stable. However, this characteristic is system-dependent and cannot be extrapolated to all CBCT systems. The long-term stability of the HU-ED calibration curve for the X-ray Volume Imaging system (XVI; Elekta AB, Stockholm, Sweden) has not yet been investigated. The objectives of the present study were to verify the stability of the HU value of the XVI system over a period of 1 year, and to evaluate the effects of variation in the HU-ED calibration curves on dose calculation.

MATERIALS AND METHODS

The XVI mounted on a Synergy linear accelerator (Elekta AB) was used for acquisition of CBCT images. The Gammex model 467 tissue characterisation phantom (Gammex Inc., Middleton, WI, USA) was scanned using the CBCT system once a month over a period of 1 year. The CBCT scan conditions were as follows: 120 kV, 40 mA, a S20 collimator, a F0 filter (no-bowtie filter) and 360° acquisition for field of view (FOV) of size S (FOV-S, 27 cm diameter); and 120 kV, 40 mA, a M20 collimator, a F1 bowtie filter and 360° acquisition for the FOV of size M (FOV-M, 41 cm diameter). The HU value for air cannot be obtained from an image set using the FOV-S because the phantom diameter of 33 cm is larger than the diameter of the FOV-S. Therefore, one of the Solid Water® (Gammex Inc., Middleton, WI, USA) insert rods was removed to create an air region where the HU values could be measured. The recommendations in the Gammex manual were followed regarding placement of the other rods (Figure 1). Regarding the FOV-M, the same phantom was scanned to match the phantom conditions with the FOV-S scan. The phantom was placed at the isocenter. HU values for each material rod on three slices around the centre slice of the phantom were measured and averaged. The beam hardening correction was applied to the HU values of the inner rods according to the Gammex manual.

The scan and measurements were repeated monthly for 1 year. The mean HU-ED calibration curves for the FOV-S and FOV-M (Smean and Mmean, respectively) were compiled from the mean HU values of the rods. HU-ED calibration curves using the mean $\pm$ twice the standard deviation were also created (S + 2SD; S − 2SD; M + 2SD; M − 2SD) to simulate

https://doi.org/10.1017/S1460396915000321 Published online by Cambridge University Press

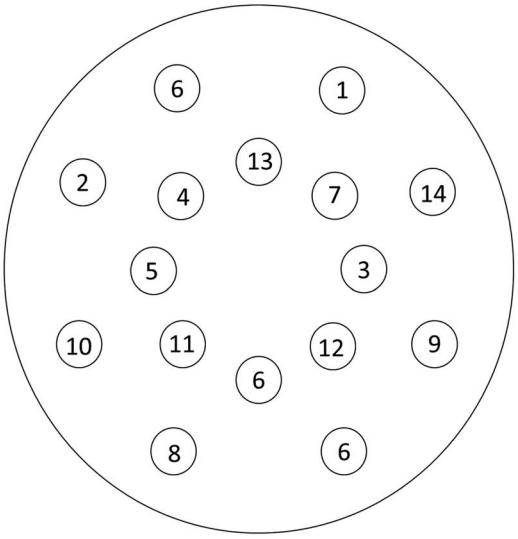

Number	Rod material	Relative electron density
1	LN-300 Lung	0.291
2	LN-450 Lung	0.473
3	AP6 Adipose	0.928
4	BR-12 Breast	0.957
5	Water insert	1.000
6	CT Solid Water	0.987
7	BRN-SR2 Brain	1.048
8	LV1 Liver	1.061
9	IB Inner Bone	1.092
10	B200 Bone mineral	1.104
11	CB2-30% CaCO3a	1.280
12	CB2-50% CaCO3a	1.471
13	SB3 Cortical Bone	1.696
14	Air	0.000

Figure 1. Materials used and placement of the rods in the tissue characterisation phantom.

possible variation. Each of the HU values above an ED of 1·0 and HU values below an ED of 1·0 were approximated using a linear function for creation of the HU-ED calibration curves. The resulting calibration curves were used to evaluate the impact on dose calculation.

Dose distributions on digital phantoms were calculated using the XiO radiation treatment planning system release 4·62 (Elekta AB). Digital phantoms of size $27 \times 27 \times 25$ and $30 \times 30 \times 25$ cm^3 were created for the FOV-S and the FOV-M, respectively. The HU value for the digital phantom was the same as the mean value for the Solid Water rod for each FOV-S and FOV-M. The voxel size of the digital phantom images for both the FOV-S and FOV-M was $1{\cdot}0 \times 1{\cdot}0 \times 1{\cdot}0$ mm^3; and was the same as that in the CBCT images for both the FOV-S and FOV-M. The reason why the digital phantoms were used for dose calculation instead of actual CBCT images was that the HU value for a CBCT image can be affected by other factors such as object volume.[7,8] This study focused on the temporal variation in the HU values. When the Solid Water slab phantom was scanned with the CBCT system, the HU values obtained differed from the mean HU value for the Solid Water rod in the tissue characterisation phantom.

X rays with energies of 6 and 10 MV generated using a Synergy BM (Elekta AB) were used for treatment planning. The treatment plan involved one port of the gantry angled at 0° and the collimator angled at 0°. A field size of $10{\cdot}2 \times 10{\cdot}2$ cm^2 was achieved using 4-mm thick multi-leaf collimators, because the Synergy BM does not have jaw collimators. The plan isocenter was placed at a depth of 10 cm and a dose of 1·0 Gy was planned to this point using the superposition algorithm. A dose profile along the central axis of the beam was obtained from each calculated dose distribution to compare the effects of variation in the HU-ED calibration curve.

RESULTS

The HU value for the higher ED rods decreased between the first and last measurements. Specifically, the HU for the SB3 cortical bone rod decreased by about 100 HU for the FOV-S and by about 300 HU for the FOV-M. HU values for the other rods, with the exception of the air space for both the FOV-S and FOV-M, the LN-450 lung rod for the FOV-M, and the LN-300 for the FOV-M showed a decreasing trend. The HU for the air space for both the FOV-S and FOV-M and for the LN-450 and LN-300 rods were stable. However, the

https://doi.org/10.1017/S1460396915000321 Published online by Cambridge University Press

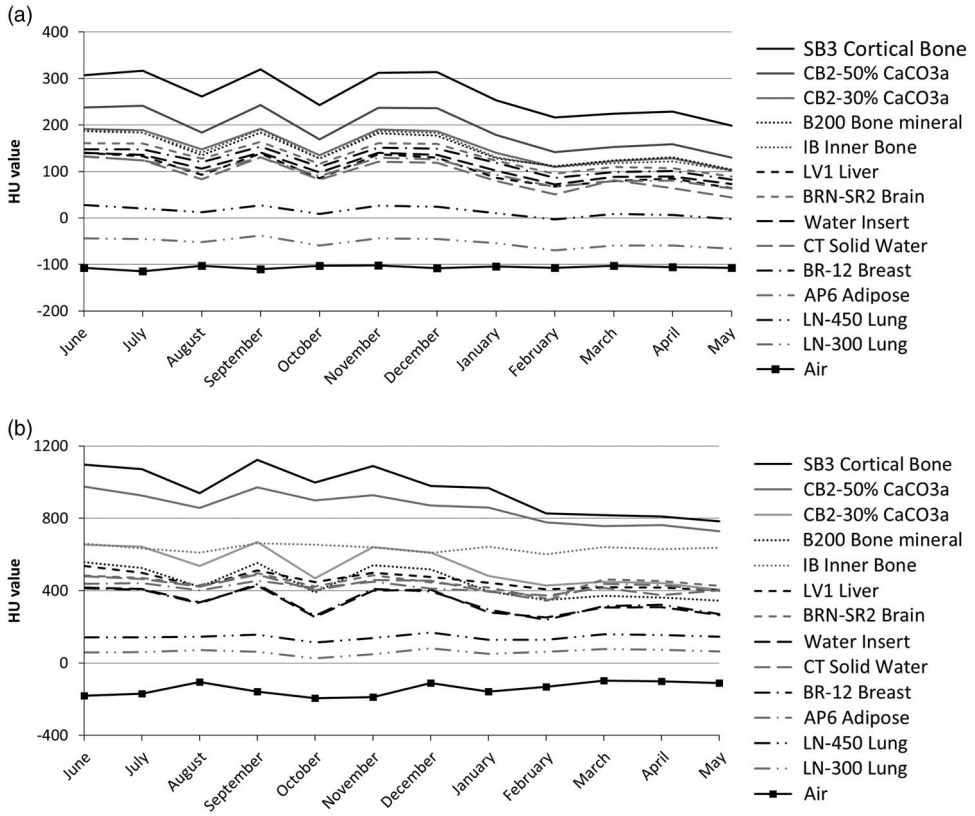

Figure 2. Variation in the HU values for the FOV-S and FOV-M. (a) The yearly variation in the HU values for the FOV-S. (b) The yearly variation in the HU values for the FOV-M.
Abbreviations: HU, Hounsfield unit; FOV-S, field of view of size S; FOV-M, field of view of size M.

decreasing trends could change the slope of the HU-ED calibration curve over the 1-year evaluation period (Figure 2). The HU values for the FOV-M measured over 1 year had larger SDs than those for the FOV-S (Figure 3). Regarding the SD for the FOV-M, the HU value for the higher ED rods had larger SDs than those for the lower ED rods.

The HU-ED calibration curves for the FOV-S and FOV-M are shown in Figure 4. The HU-ED calibration curve for the FOV-S was steeper than that for the FOV-M. Because almost all of the standard deviations of the HU values for the FOV-M were larger than those for the FOV-S, the M + 2SD and M − 2SD HU-ED calibration curves exhibited greater divergence from the Mmean calibration curve than was the case for the S + 2SD and S − 2SD HU-ED calibration curves.

Regarding the dose profiles of the 6 and 10 MV photon beams for the FOV-S, those for the HU-ED calibration curves of S + 2SD and S − 2SD had different slopes compared with the profiles of the 6 and 10 MV beams for the HU-ED calibration curve for the Smean. The slope of the dose profile for the S + 2SD curve was more gradual than that for the Smean, and the slope of the dose profile for the S − 2SD curve was steeper. The profile for the S + 2SD curve involved a lower dose than that for the Smean curve until a depth of 10 cm, and the profile for the S − 2SD curve involved a higher dose. The maximum dose for the Smean curve was 148·0% for the 6 MV beam and 138·2% for the 10 MV beam. The maximum dose for the S + 2SD curve was 138·9% (−9·1%) and 129·8% (−8·4%) for the 6 and 10 MV beams, respectively. The maximum dose for the S − 2SD curve was 165·8% (+17·8%) and 153·8% (+15·6%) for the 6 and 10 MV beams, respectively (Figures 5a and 5b).

Regarding the profiles for the FOV-M, the profiles for the M + 2SD and M − 2SD curves

https://doi.org/10.1017/S1460396915000321 Published online by Cambridge University Press

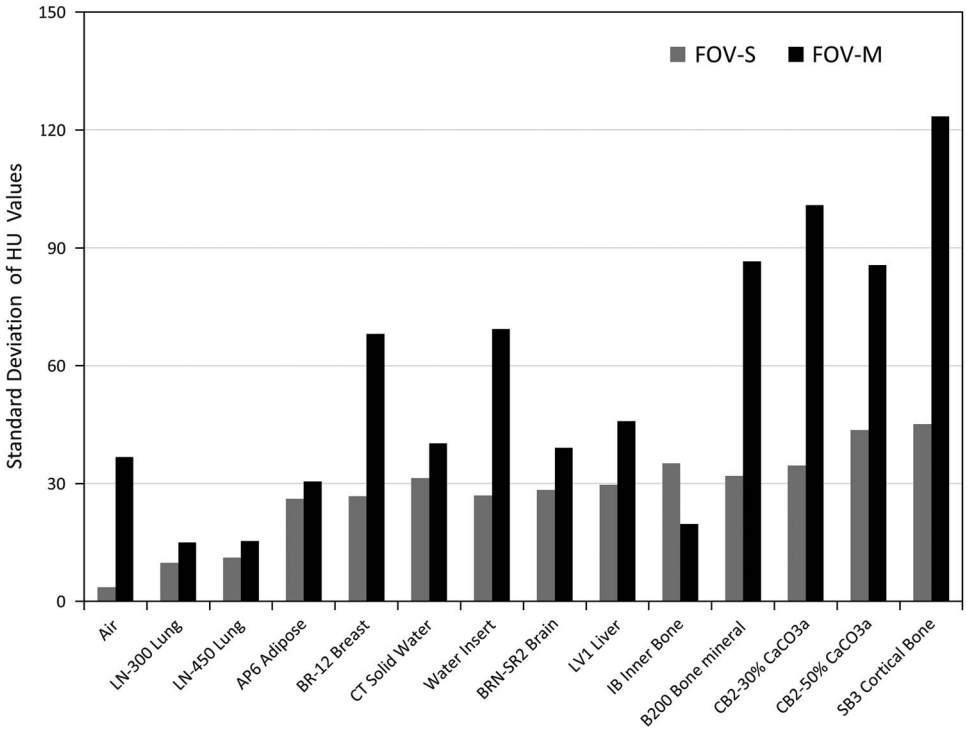

Figure 3. Standard deviation of the HU values for the material rods measured over a 1-year period.
Abbreviation: HU, Hounsfield unit.

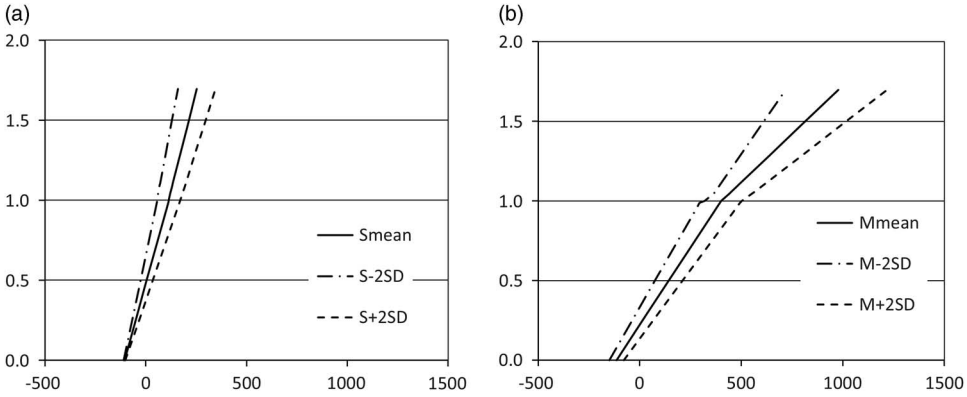

Figure 4. HU-ED calibration curves for the FOV-S and FOV-M. (a) The HU-ED calibration curves for the FOV-S. (b) The HU-ED calibration curves for the FOV-M.
Abbreviations: HU-ED, Hounsfield unit to relative electron density; FOV-S, field of view of size S; FOV-M, field of view of size M.

had a different slope compared with the profile for the Mmean curve, as well as the profiles for the FOV-S. The maximum dose for the Mmean curve was 147·9% for the 6 MV beam and 137·9% for the 10 MV beam. The maximum dose for the M + 2SD curve was 140·0% (−7·9%) and 130·3% (−7·6%) for the 6 and 10 MV beams, respectively, the maximum dose for the M-2SD curve was 165·8% (+17·8%) and 153·8% (+15·6%) for the 6 and 10 MV beams, respectively (Figures 5c and 5d). The differences of the maximum doses for the S ± 2SD compared with that for the Smean were larger than those for the M ± 2SD and Mmean.

https://doi.org/10.1017/S1460396915000321 Published online by Cambridge University Press

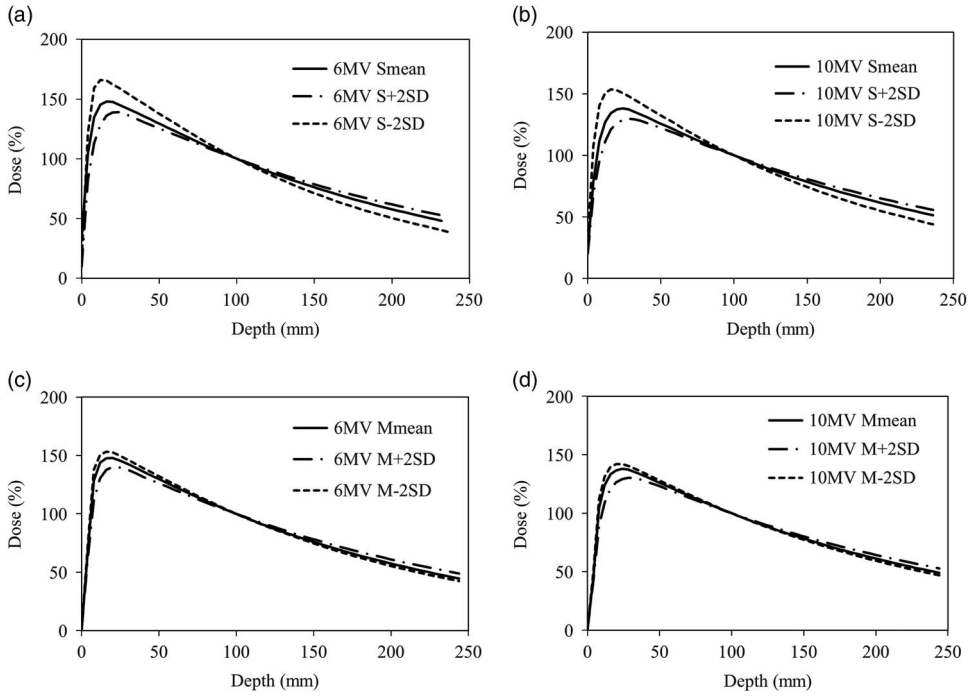

Figure 5. Dose profiles in the digital phantoms. (a) Profiles for the FOV-S using 6 MV X rays. (b) Profiles for the FOV-S using 10 MV X rays. (c) Profiles for the FOV-M using 6 MV X rays. (d) Profiles for the FOV-M using 10 MV X rays. Abbreviations: FOV-S, field of view of size S; FOV-M, field of view of size M.

DISCUSSION

In the present study, a trend in HU values was found over the 1-year period. Specifically, the HU values of the high ED rods decreased over time. The overall difference between the first scan and the final scan for these rods was about 100 HU for FOV-S and about 300 HU for FOV-M. The standard deviation of voxel values in measured regions of interest for the high ED rods was about 20 HU for FOV-S and about 90 HU for FOV-M. The overall decrement was larger than the maximum standard deviations. Possible reasons for this trend are changes in output from the X-ray tube and changes in the sensitivity of the flat-panel detector (FPD). The X-ray tube was replaced during the period of study. The results from April and May were obtained after the tube replacement and the HU values were almost the same as those obtained in March before the tube was replaced. The X-ray output was also checked by a maintenance technician employed by the manufacturer after the tube replacement. Thus, changes in X-ray output were not the factor responsible for the trends observed with the HU values. Instead, the trend in HU values may have resulted from a change in sensitivity of the FPD. For comparison with this study, Hu et al.[4] verified the stability of HU values over the course of 3 months and they observed a maximum change in HU of 21. However, 3 months is a relatively short period for evaluation of trending in HU values.

For the FOV-M, the HU values of the IB Inner Bone rod were larger than those of the CB2-30% CaCO3a rod and the B200 Bone mineral rod (Figure 2b). The HU value of the IB Inner Bone rod should be lower than those of the CB2-30% CaCO3a rod and the B200 Bone mineral rod as well as lower than the results obtained for the FOV-S based on their ED values. This shift in HU values resulted in a fluctuation of the HU-ED calibration curve. However, such fluctuations in HU-ED calibration curves are often observed with general CT systems.[4,11] Cheng et al.[11] compared HU-relative stopping power curves of several CT systems based on HU values. They found that the fluctuation in relative HU-stopping power

https://doi.org/10.1017/S1460396915000321 Published online by Cambridge University Press

curves occurred around the relative ED value of 1·0. At relative ED values of <1·2, the relative stopping power was almost the same as the relative ED. This study used a bowtie filter for the CBCT scans with FOV-M. This filter changes the X-ray spectrum of the CBCT and is likely the reason for fluctuations of the HU-ED calibration curve observed with the FOV-M.

The HU-ED calibration curve for the FOV-S was steeper than that for the FOV-M, and both of the HU-ED calibration curves were also steeper than that typically observed with a general CT system. This phenomenon occurs because the HU value of CBCT scanners is not a true HU value based on the attenuation coefficient of water. The HU values of CBCT scanners are dependent on scan conditions such as X-ray tube voltage and current. Thus, HU-ED calibration curves for all the CBCT conditions expected to be used need to be obtained for accurate dose calculations on CBCT images.

In addition, dose distributions calculated using a steep HU-ED calibration curve can be very sensitive to variations in the HU values caused by image noise or artifact. In this study, the difference in dose calculated using the Smean and the S + 2SD or S − 2SD curves was larger than the difference in dose between the Mmean and the M + 2SD or M − 2SD curves. A maximum deviation of 17·8% occurred in the dose calculated with the S − 2SD curve owing to the steeper HU-ED calibration curve. For the FOV-S, an ED of about 0·8 and 1·4 was applied to the digital phantom in the HU-ED conversion in dose calculations for the S + 2SD and S − 2SD curves, respectively. Regarding the FOV-M, an ED of about 0·9 and 1·1 was applied in dose calculations involving the M + 2SD and M − 2SD, respectively. The true ED for Solid Water is 0·987. The HU-ED calibration curve for CBCT systems are typically steeper than those for a general CT system and impact radiotherapy treatment planning. Dose calculations using CBCT images will be more sensitive to noise and artifacts than dose calculations made on planning CT images.

Consequently, if CBCT images are to be used for dose calculation in the clinical practice (such as adaptive radiotherapy), a HU-ED calibration curve for the CBCT scanner should be obtained periodically because as variations in HU values can affect dose calculations. In addition, the object volume and CBCT scan conditions can affect the HU values.[7,8] Therefore, a stabilisation method for the long-term stability of the HU value and a HU value correction method for dependency on volume and CBCT conditions should be applied to the CBCT images for dose calculation.

CONCLUSION

HU values for each ED rod varied over a 1-year period, with a trend and possible variations in the HU-ED calibration curve producing a ≤17·9% difference in the maximum dose in a one port treatment plan. Thus, if CBCT images will be used for dose calculation, a HU-ED calibration curve should be obtained periodically.

Acknowledgement

None.

Financial Support

This work was supported by JSPS KAKENHI grant number 26460724.

Conflicts of Interest

None.

References

1. Veiga C, McClelland J, Moinuddin S et al. Toward adaptive radiotherapy for head and neck patients: feasibility study on using CT-to-CBCT deformable registration for "dose of the day" calculations. Med Phys 2014; 41 (3): 031703.
2. Boggula R, Lorenz F, Abo-Madyan Y et al. A new strategy for online adaptive prostate radiotherapy based on cone-beam CT. Z Med Phys 2009; 19 (4): 264–276.
3. Nijkamp J, Pos F J, Nuver T T et al. Adaptive radiotherapy for prostate cancer using kilovoltage cone-beam computed tomography: first clinical results. Int J Radiat Oncol Biol Phys 2008; 70 (1): 75–82.
4. Hu W, Ye J, Wang J, Ma X, Zhang Z. Use of kilovoltage X-ray volume imaging in patient dose calculation for head-and-neck and partial brain radiation therapy. Radiat Oncol 2010; 5 (29): 1–10.

https://doi.org/10.1017/S1460396915000321 Published online by Cambridge University Press

5. Ping H S, Kandaiya S. The influence of the patient size and geometry on cone beam-computed tomography Hounsfield unit. J Med Phys 2012; 37 (3): 155–158.
6. Guan H, Dong H. Dose calculation accuracy using cone-beam CT (CBCT) for pelvic adaptive radiotherapy. Phys Med Biol 2009; 54 (20): 6239–6250.
7. Hatton J, McCurdy B, Greer P B. Cone beam computerized tomography: the effect of calibration of the Hounsfield unit number to electron density on dose calculation accuracy for adaptive radiation therapy. Phys Med Biol 2009; 54 (15): N329–N346.
8. Rong Y, Smilowitz J, Tewatia D, Tomé W A, Paliwal B. Dose calculation on kV cone beam CT images: an investigation of the HU-density conversion stability and dose accuracy using the site-specific calibration. Med Dosim 2010; 35 (3): 195–207.
9. Onozato Y, Kadoya N, Fujita Y et al. Evaluation of on-board kV cone beam computed tomography-based dose calculation with deformable image registration using Hounsfield unit modifications. Int J Radiat Oncol Biol Phys 2014; 89 (2): 416–423.
10. Yadav P, Ramasubramanian V, Paliwal B R. Feasibility study on effect and stability of adaptive radiotherapy on kilovoltage cone beam CT. Radiol Oncol 2011; 45 (3): 220–226.
11. Cheng C, Zhao L, Wolanski M et al. Comparison of tissue characterization curves for different CT scanners: implication in proton therapy treatment planning. Transl Cancer Res 2013; 1 (4): 236–246.

https://doi.org/10.1017/S1460396915000321 Published online by Cambridge University Press